

Research



Cite this article: Tomašových A *et al.* 2020 Ecological regime shift preserved in the Anthropocene stratigraphic record. *Proc. R. Soc. B* **287**: 20200695.
<http://dx.doi.org/10.1098/rspb.2020.0695>

Received: 27 March 2020

Accepted: 23 May 2020

Subject Category:

Palaeobiology

Subject Areas:

palaeontology, ecology

Keywords:

conservation palaeobiology, stratigraphic palaeobiology, stasis, regime shift, time averaging, northern Adriatic Sea

Author for correspondence:

Adam Tomašových

e-mail: geoltoma@savba.sk

Electronic supplementary material is available online at <https://doi.org/10.6084/m9.figshare.c.5007803>.

Ecological regime shift preserved in the Anthropocene stratigraphic record

Adam Tomašových¹, Paolo G. Albano², Tomáš Fuksi¹, Ivo Gallmetzer², Alexandra Haselmair², Michał Kowalewski³, Rafał Nawrot², Vedrana Nerlović⁴, Daniele Scarponi⁵ and Martin Zuschin²

¹Earth Science Institute, Slovak Academy of Sciences, Dúbravská cesta 9, 84005 Bratislava, Slovakia

²Department of Palaeontology, University of Vienna, Althanstrasse 14, 1090 Vienna

³Florida Museum of Natural History, University of Florida, 1659 Museum Road, Gainesville, FL 32611, USA

⁴Department of Marine Studies, University of Split, Ruđera Boškovića 37, 21000 Split, Croatia

⁵Department of Biological, Geological and Environmental Sciences, University of Bologna, Piazza di Porta San Donato 1, I-40126 Bologna, Italy

AT, 0000-0002-0471-9480; PGA, 0000-0001-9876-1024; MK, 0000-0002-8575-4711; RN, 0000-0002-5774-7311; VN, 0000-0001-9799-2066; DS, 0000-0001-5914-4947; MZ, 0000-0002-5235-0198

Palaeoecological data are unique historical archives that extend back far beyond the last several decades of ecological observations. However, the fossil record of continental shelves has been perceived as too coarse (with centennial-millennial resolution) and incomplete to detect processes occurring at yearly or decadal scales relevant to ecology and conservation. Here, we show that the youngest (Anthropocene) fossil record on the northern Adriatic continental shelf provides decadal-scale resolution that accurately documents an abrupt ecological change affecting benthic communities during the twentieth century. The magnitude and the duration of the twentieth century shift in body size of the bivalve *Corbula gibba* is unprecedented given that regional populations of this species were dominated by small-size classes throughout the Holocene. The shift coincided with compositional changes in benthic assemblages, driven by an increase from approximately 25% to approximately 70% in median per-assemblage abundance of *C. gibba*. This regime shift increase occurred preferentially at sites that experienced at least one hypoxic event per decade in the twentieth century. Larger size and higher abundance of *C. gibba* probably reflect ecological release as it coincides with an increase in the frequency of seasonal hypoxia that triggered mass mortality of competitors and predators. Higher frequency of hypoxic events is coupled with a decline in the depth of intense sediment mixing by burrowing benthic organisms from several decimetres to less than 20 cm, significantly improving the stratigraphic resolution of the Anthropocene fossil record and making it possible to detect sub-centennial ecological changes on continental shelves.

1. Introduction

Although high-resolution time series based on monitoring of living assemblages (LAs) can directly detect the dynamics of marine ecosystem responses to natural or anthropogenic stressors [1–4], their duration is typically decadal [5,6]. This temporal extent limits their ability to detect former baseline states or discriminate short-term fluctuations from sustained regime shifts (i.e. a large, abrupt and persistent shift in ecosystem structure, [7]). By contrast, stratigraphic records that archive much longer time series can successfully detect long-term ecosystem shifts driven by pollution, deoxygenation, eutrophication or overfishing that occurred over the past centuries or millennia [8–12]. These changes can be comparable in magnitude to those that occurred during ecological crises associated with mass extinctions [13–15]. However, determining whether the ecological changes were gradual or abrupt on the basis of the stratigraphic record is hindered by

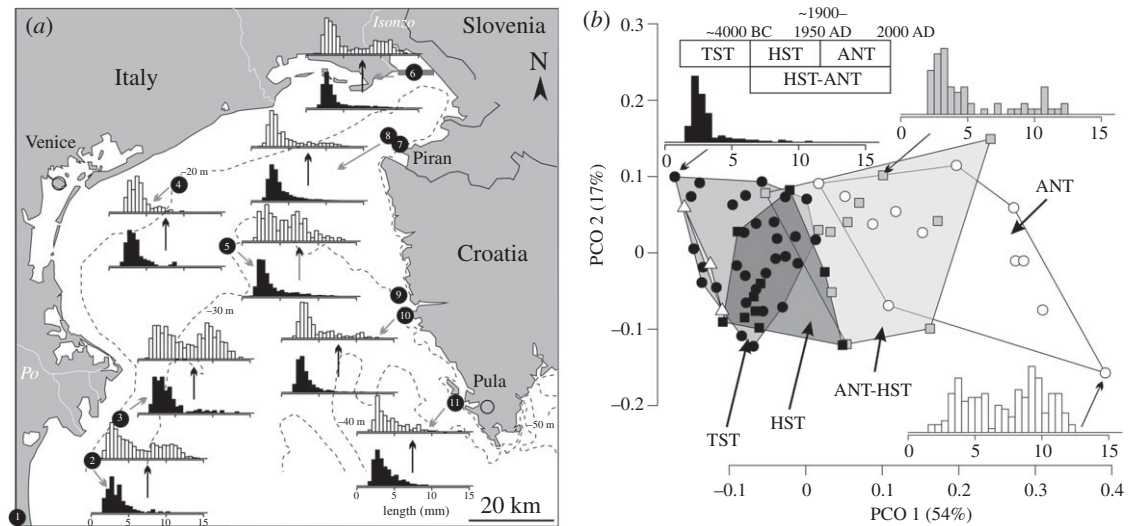


Figure 1. Size distributions of *C. gibba* in Holocene transgressive (TST) and highstand (HST) assemblages, and in Anthropocene (twentieth century) death assemblages (DAs) in the northern Adriatic Sea. (a) Holocene–Anthropocene site pairs based on eight selected sites show that right-skewed and thin-tailed HST assemblages (black) are replaced by bimodal (under low time averaging) or heavy-tailed (under high time averaging) Anthropocene assemblages (white). The labels summarize sites analysed in this study: 1, Po Plain core S10; 2, Po 4; 3, Po 3; 4, Venice; 5, site D2; 6, Bay of Panzano (transect with seven Van Veen grab sites and two sites with sediment cores); 7, Piran 1; 8, Piran 2; 9–10, Rovinj 120 and 38; 11, Brijuni. The shift in size structure at sites with high time averaging (sites 5 and 10) is based on shells with (white) and without (black) periostracum. (b) The size structure of *C. gibba* differs between Holocene (TST and HST) and Anthropocene (ANT) assemblages at sites greater than 8 m water depth (white circles), and at sites less than 8 m depth (white triangles) in principal coordinate analysis (PCO) analysis based on 10–30 cm-thick increments. The highstand–Anthropocene (HST–ANT) assemblages at sites with high time averaging are based on shells with periostracum (grey squares).

hiatuses (induced by erosion and non-deposition) and time averaging (mixing of non-contemporaneous generations) [16,17], unless bioturbation is limited and erosion is rare or episodic as in lacustrine, hypersaline or anoxic environments [18–20]. As a result, benthic fossil assemblages from continental shelves—settings that provide the bulk of the deep-time palaeontological data on ecological dynamics—are incomplete and temporally mixed over 10^2 – 10^4 year time scales [21]. The hiatuses and time averaging of bioturbated sediments can result in a fossil record that underestimates the magnitude of ecological change over a given timespan [22,23]. Conversely, hiatuses can produce stratigraphic patterns mimicking abrupt ecological shifts occurring over a short stratigraphic distance even when the actual pace of ecosystem change was gradual [24], further confounding assessments of ecological turnover on the basis of stratigraphic records.

The Holocene record provides a unique testing opportunity for assessing whether the response of marine ecosystems to gradual or abrupt pressures can be resolved from stratigraphic records. Absolute dating of multiple shells embedded in sediment cores allows reconstructing the chronological record regardless of time averaging (i.e. fossils can be aligned into a time series independently of their stratigraphic position) and contrasting it against the stratigraphic record (i.e. fossils are assigned to the mean age of a sedimentary layer in which they are embedded). Here, we test whether the responses of benthic communities to eutrophication and hypoxic events in the Adriatic Sea that intensified during the late twentieth century (figure 1a) are detectable in the Anthropocene stratigraphic record (informally denoting here the twentieth and twenty-first centuries). Specifically, we (i) assess chronologic and stratigraphic changes in body size of an opportunistic, hypoxia-tolerant bivalve (*Corbula gibba*) collected in sediment cores, and (ii) compare composition of pre-twentieth century Holocene mollusc assemblages with Anthropocene assemblages. Our results demonstrate that bioturbated sediment cores can generate high-resolution archives of

ecological changes induced by hypoxia, which can suppress sediment mixing by burrowing organisms and, consequently, enhance the temporal resolution of the resulting fossil record.

To identify regime shifts, we focus on body size because this attribute tracks ecosystem changes during natural [25,26] and anthropogenic disturbances [27] and predicts present-day extinction risks for marine molluscs [28]. We combine body size estimates based on valve length of the infaunal bivalve *C. gibba* from death assemblages (DAs) collected in sediment cores and Van Veen grabs with formerly published estimates of time averaging based on radiocarbon-calibrated amino acid racemization (AAR; figure 2, see the electronic supplementary material and the Dryad Digital Repository: <https://doi.org/10.5061/dryad.t4b8gthzr> [29]). First, we quantify the pattern and timing of shift in body size in chronological and stratigraphic records using the threshold regression [30] and models assessing their directionality [31,32]. Second, we evaluate the sensitivity of the preserved stratigraphic record of a regime shift to increasing time averaging. Third, we assess whether the shifts in body size covary with estimates of relative frequency of seasonal hypoxia and whether they coincide with compositional changes in molluscan communities.

2. Methods

(a) Sediment cores and time averaging

DAs of *C. gibba* were collected in sediment cores and Van Veen grabs in the northern Adriatic Sea. First, 1.5 m long piston cores were collected at eight sites at water depths between 10 and 44 m in 2013 (two sites at the Po prodelta, two sites at the Isonzo prodelta, two sites off Piran and one site at Venice and Brijuni). Second, the 26 m long Holocene succession of the S10 core was drilled near Comacchio (Po coastal plain; [33]). Third, Van Veen grabs (approx. upper 10 cm of the sediment column) were collected at 14 sites at Po prodelta (two sites), off Venice (two sites), off Rovinj (two sites) and in the Bay of Panzano (Isonzo prodelta) (eight sites) (electronic

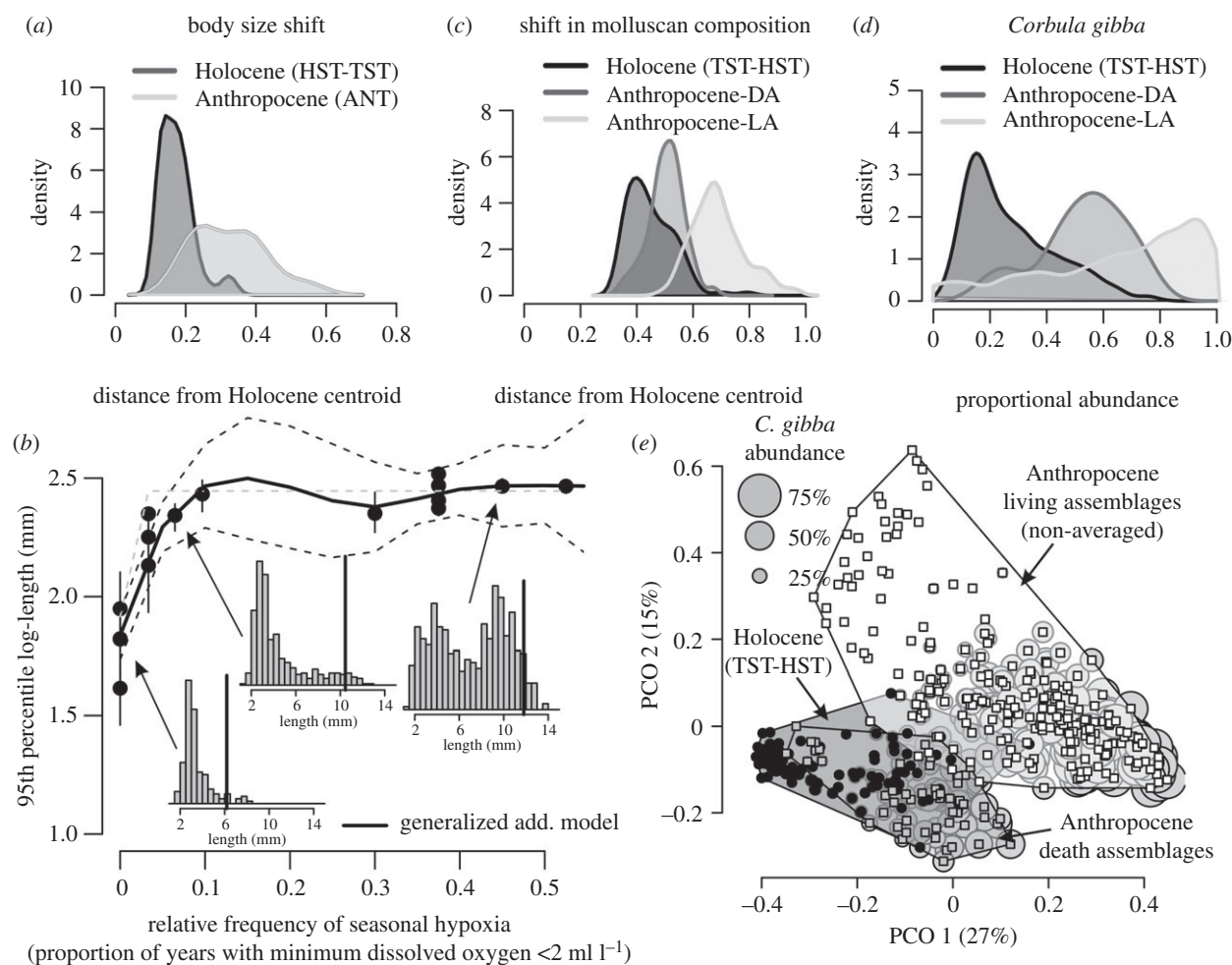


Figure 2. The size and compositional regime shift between Holocene and Anthropocene assemblages and the effect of frequency of hypoxic events on shell size of *C. gibba*. (a) Density kernels show that the Fréchet distances from the Holocene centroid to Anthropocene assemblages (light grey) exceed those between Holocene assemblages and their centroid (dark grey). (b) The relationship between the 95th percentile log-length of *C. gibba* in DAs (based on specimens with periostracum only) and the relative frequency of seasonal hypoxia between 1980 and 2010 points to an abrupt nonlinear increase in size when a seasonal hypoxic event occurs at least once per decade. (c) Compositional overlap between Holocene and Anthropocene assemblages: density kernels show that the Bray–Curtis distances from the Holocene centroid to Anthropocene living assemblages (LAs; light grey) are larger than those among the Holocene death assemblages (dim grey). Anthropocene death assemblages (DAs; dark grey) have intermediate position. (d) The distribution of *C. gibba* relative abundance, with less than 20% in Holocene assemblages and greater than 90% in Anthropocene LAs. (e) Genus-level compositional separation between Holocene (TST and HST), Anthropocene DAs and Anthropocene LAs in principal coordinate analysis (PCO). The size of the bubble plots is scaled to abundance of *C. gibba* relative to abundance of all molluscs.

supplementary material, figure S1). Estimates of increment median ages, sedimentation rates and time averaging were based on shell ages (AAR calibrated by ^{14}C) of four molluscan species [34–39]. Time averaging corresponds to an inter-quartile age range in years (IQR) in approximately 10–30 cm thick units [34–37,40,41]. Net sedimentation rate was approximately 0.3 cm y^{-1} during the transgressive phase (TST) and $1\text{--}2 \text{ cm y}^{-1}$ during the highstand phase (HST) at the Po prodelta, $0.2\text{--}0.4 \text{ cm y}^{-1}$ during the HST at the Isonzo prodelta, and approximately 0.01 cm y^{-1} during the TST and HST off Istria and in the Gulf of Venice [34–37,40,41]. The uppermost sediment core increments corresponding to twentieth–twenty-first centuries do not show any signs of change in the sedimentation rate [34]. These differences in net sedimentation rates partly translate to differences in time averaging. First, highly time-averaged assemblages (IQR = approx. 1000–2000 years) occur in TST (cores from the Po Plain, Venice, Piran and Brijuni) and HST increments (Venice, Piran, Brijuni), including mixtures of highstand and Anthropocene shells in topcore and surface DAs at Rovinj, Venice, Piran and Brijuni. Second, weakly time-averaged assemblages (IQR = approx. 10–200 years) occur in HST and Anthropocene increments of the cores from Po and Isonzo prodeltas. These cores at Po and Isonzo prodeltas show a significant decline in time averaging in post-nineteenth century increments from 10^1 to 10^0 and from 10^2 to 10^1 years, respectively [34].

(b) Size data

We measured shell size with the length of right valves in 20 774 specimens of *C. gibba*. Chronological analyses of length distributions are based on specimens from two Po cores that were directly dated [34] and were partitioned into 5 year age cohorts (electronic supplementary material, table S1 and S2). Stratigraphic analyses of length distributions are performed (i) at the scale of 5–10 cm thick increments in cores and (ii) by pooling these increments into 10–30 cm thick units characterized by homogeneous sedimentologic composition (72 units in total). Moreover, the analyses are also performed at two spatial scales, including (i) pooling closely located sites into three localities (Po, Isonzo, Piran), and (ii) at the scale of eight individual sites (electronic supplementary material, table S1, S3 and S4). Size data are available in the electronic supplementary material, S2.

(c) Multivariate size analyses

We assessed whether size structure underwent a shift in the twentieth century to a new state, using principal coordinate analysis (PCO), with the Fréchet distances between 10 and 30 cm thick units, based on proportional abundances of 1 mm cohorts (electronic supplementary material, figure S2A and B). All units are

assigned to four stratigraphic intervals, including (i) TST (between 10–7 kyr cal BP), (ii) HST, here referring to increments deposited prior to the late twentieth century, (iii) Van Veen grabs and topcore samples (uppermost 10–20 cm) with a strongly time-averaged mixture of the HST and post-nineteenth-century sediments deposited under less than 0.01 cm y^{-1} (HST-Anthropocene), and (iv) the topcore samples at Po and Isonzo prodeltas deposited under greater than 0.2 cm y^{-1} and corresponding to the Anthropocene. We modified analogue matching analyses to assess whether size-frequency distributions of Anthropocene *Corbula* populations represent a novel state, i.e. whether they extend beyond the variation defined by all Holocene (TST and HST) *Corbula* populations. These analyses evaluate whether Fréchet distances between the Holocene centroid and Anthropocene assemblages exceed distances between the Holocene centroid and Holocene assemblages ([38,39,42], electronic supplementary material, S3 and S4). We evaluated differences in size structure between four stratigraphic units with permutational multivariate analysis of variance (PERMANOVA, [43]). Periostracum is usually not preserved on *C. gibba* valves older than 100 years (electronic supplementary material, figure S3), so the mixing of the twentieth century specimens with much older shells in topcore HST-Anthropocene units can be minimized by analysing valves with periostracum only. Therefore, PCO is based on 72 units (exhaustive analyses based on all specimens of *C. gibba*) and on 66 units including only valves with periostracum.

(d) Detection of regime shifts

We assessed whether the abrupt shift in (i) the mean and (ii) the 95% percentile log-length detected in the chronological records is also preserved in the stratigraphic records. The mean length captures the central tendency across the whole size-frequency distribution, including juvenile specimens, whereas the 95% percentile length is informative about the size-frequency distribution of adult individuals. We use three approaches to detect the regime shift, here approximated by changes in the shape of the size-frequency distribution of *C. gibba*, one of the most abundant molluscan species. First, a threshold regression identifies abrupt shifts in size and their timing in chronological or stratigraphic time series. We use an F statistic that evaluates whether the model with one shift explains significantly more than the model with just an intercept [30], and the adjusted R^2 to compare the threshold model with a simple linear model. Second, we fit chronological or stratigraphic series of size to models [31] that allow for one abrupt shift between two segments characterized by either unbiased random walk, stasis or directional trends (eight models in total, we set the minimum segment length to seven increments; electronic supplementary material, table S3 and S4). The stasis model is considered as uncorrelated, normally distributed variation in size (either in the mean or in the 95th percentile log-length), with temporal variance ω around a long-term mean θ . Size is expected to converge immediately to θ from any precursor (ancestral) value. Directional trend is modelled as a change in size at each time step drawn from a normal distribution of size changes, with non-zero mean μ_s and a variance σ_s^2 . A random walk is a special case of the directional trend in which $\mu_s = 0$. The punctuation model refers to one abrupt shift separated by two segments of stasis with θ_1 and θ_2 and a single ω , and is thus equivalent to the definition of the regime shift. Third, we assess the effect of time averaging (i) on the model support for the punctuation model and (ii) on temporal variability in size (ω of the stasis model).

(e) Covariates of size shifts

We assess the response of the mean and the 95th percentile log-length to a hypothesized driver—the relative frequency of seasonal hypoxia (the number of years with minimum dissolved

oxygen concentrations less than 2 ml l^{-1} , or less than approximately 3 mg l^{-1} [38] relative to the total number of years based on measurements in 1980–2010 at 16 sites, see the electronic supplementary material, S1)—with rank correlations and generalized additive models. We also compare the taxonomic composition of the Holocene (TST and HST) molluscan assemblages (deposited prior to the twentieth century or during the earliest twentieth century; 95 assemblages from the cores used in the analyses of shell size) with 54 Anthropocene DAs (late twentieth century deposits from the uppermost core increments) and 223 Anthropocene LAs collected since 1980s (data compiled from published sources). LAs are based on Van Veen grab samples collected in multiple studies of soft-bottom habitats in the Po prodelta and in the Gulf of Trieste between 10–30 m water depth and are thus standardized to genus level. Compositional differences are analysed with PCO, PERMANOVA (Bray–Curtis distances based on square-root transformed proportional abundances of genera), and with the modified analogue matching by evaluating whether Anthropocene assemblages extend beyond the variation defined by the Holocene assemblages (using Bray–Curtis distances [39,42–44]).

(f) Sensitivity of the stratigraphic expression of regime shifts to time averaging

In simulations, we assess how the support for the punctuation model changes and how the volatility in size declines in the stratigraphic record as time averaging increases from 1 up to 1000 years when compared to the true chronological pattern produced by the regime shift (i.e. punctuation separated by two stasis segments). We simulate the effects of time averaging (i) on the timing and the abruptness of the shift and (ii) on the estimate of temporal variance in the mean and in the 95th percentile log-length (ω) with two scenarios. In a first scenario, we assess the sensitivity of ω in a stasis model with $\theta_1 = 1$ in a Holocene-scale simulation with duration of 10 000 years, varying true ω between 0.01 and 0.2 (values comparable to empirical estimates). In a second scenario, tailored to the past 200 years to capture sedimentation conditions at Po and Isonzo prodeltas, the abrupt increase in size from $\theta_1 = 1$ (2.7 mm) to $\theta_2 = 2$ (7.4 mm) occurs in 1950 and the true ω of non-averaged time series is set to 0.01. In both scenarios, we sample 50 individuals in each of the thirty increments (comparable to the number of increments and sample sizes in 1.5 m cores) and fit time-averaged stratigraphic series to eight size models with the same methods as empirical chronological series. We repeat simulations 1000 times, estimate means of ω in Holocene-scale simulations and compute model-specific Akaike weights in Anthropocene simulations (electronic supplementary material, S5).

3. Results

(a) Size shift in the northern Adriatic Sea

The size structure of *C. gibba* in Anthropocene assemblages (figure 1b) does not overlap with TST (10–7 kyr cal BP) and HST (approx. 7 kyr cal BP up to the nineteenth century) assemblages in PCO (figure 1b; electronic supplementary material, table S5), and 50% of Anthropocene assemblages are farther from the Holocene centroid in terms of the Fréchet distances than 97.5% of Holocene assemblages (figure 2a). TST and HST increments do not differ in size structure and are both characterized by right-skewed, thin-tailed distributions dominated by individuals less than 5 mm (figure 1a). Anthropocene assemblages from high sedimentation sites (greater than 0.2 cm y^{-1}) with centennial to decadal time averaging at the Po and Isonzo prodeltas are characterized by bimodal

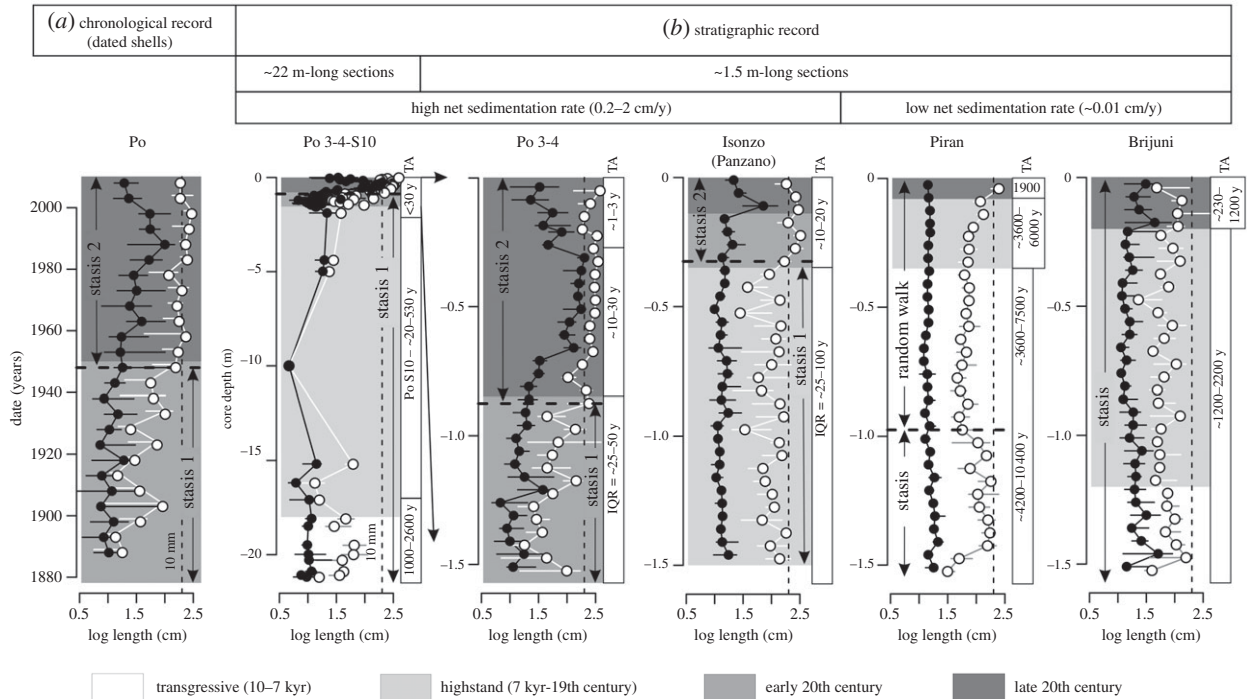


Figure 3. Chronological and stratigraphic records in the mean (black points) and the 95th percentile log-length (white points) of *Corbula gibba* and the corresponding likelihood models for temporal changes in the 95th percentile log-length. The punctuational shift in shell size in the chronological record either translates to stratigraphic punctuation at sites with relatively high sedimentation and reduced bioturbation (at Po and Isonzo) or to strongly muted stratigraphic records at sites with very slow sedimentation (at Piran and Brijuni). The chronological record is based on dated shells partitioned into 5 year cohorts at Po (a). The stratigraphic records are based on 5–10 cm thick increments at five sites (b). The 1.5 m long cores capturing the last approximately 150 years (Po 3 and Po 4) are shown separately and together with the 26 m long core S10, which extends the record to the onset of the Holocene transgression (the last 10 kyr). Thin vertical dashed lines demarcate the shell length at 10 mm. Error bars refer to 95% bootstrapped confidence intervals. Time averaging (TA) refers to the inter-quartile age range (IQR) in years.

distributions with abundant large individuals (greater than 10 mm; figure 1a). Low sedimentation sites with millennial time averaging generated by mixing of Anthropocene and HST assemblages show heavy-tailed distributions, with individuals greater than 5 mm being moderately frequent (figure 1a). The shift between the Holocene (TST and HST) and Anthropocene assemblages is thus driven by the appearance of abundant individuals greater than 10 mm in length. The mean and the 95th percentile log-length of *C. gibba* in 16 DAs correlate positively with the proportion of years with at least one hypoxic event at each of these sites (Spearman r (mean) = 0.91, $p = 0.005$, r (95th percentile) = 0.82, $p < 0.0001$). The 95th percentile log-length increases abruptly at frequency of hypoxia equal to approximately 0.1 (one year with hypoxic event per decade, figure 2b), suggesting that even a sporadic hypoxia can be sufficient for the switch from the right-skewed to the bimodal size distribution.

(b) Compositional shift in the northern Adriatic Sea

The size shift stratigraphically coincides with a major change in the molluscan community composition. The Bray–Curtis distances show that 82% of Anthropocene LAs are farther from the Holocene centroid than 97.5% of Holocene assemblages (figure 2c). The abundance of *C. gibba* increases from approximately 20 to 30% (95% confidence intervals on the median relative abundance per sample) in TST and HST increments to 50–60% in time-averaged Anthropocene DAs and to 63–75% in Anthropocene LAs (figure 2d). Higher abundance of *C. gibba* in soft-bottom habitats is associated with an increase in abundance of deposit feeders (from 7 to 22%, driven mainly

by the infaunal bivalve *Nucula*). It is compensated by the declines in abundance of the suspension-feeding gastropod *Turritellinella tricarinata* (from 20% to 1.5%, excluding *Corbula*), commensals (bivalves *Kurtiella* from 20% to 8% and *Musculus* from 3% to less than 1%), drilling gastropods (*Euspira*) and scavengers (*Tritia*) (electronic supplementary material, figure S7, electronic supplementary material, S6). PCO and PERMANOVA show that the overlap between Anthropocene assemblages and Holocene assemblages is negligible (figure 2e). However, Anthropocene LAs and DAs also strongly differ in their composition (figure 2e, electronic supplementary material, table S5).

(c) Chronological and stratigraphic record of size shifts

Threshold regressions and models assessing the directionality of trends show that chronological records in size at Po prodelta are best explained by an abrupt punctuational increase in the mean log-length (from $\theta_1 = 1.07$ to $\theta_2 = 1.53$, with $\omega = 0.007$) and in the 95th percentile log-length (from $\theta_1 = 1.6$ to $\theta_2 = 2.3$, with $\omega = 0.022$) that occurred within a single decade at approximately 1950 AD (figures 3a and 4a). This shift separates populations exhibiting stasis prior to and after 1950 AD (right-skewed and bimodal distributions, respectively). Stratigraphic records at sites with high sedimentation (greater than 0.2 cm y^{-1}) at Po and Isonzo prodeltas also support a single abrupt shift both in the mean and the 95th percentile log-length (in the mid-twentieth century at 80–110 cm core depth at Po and in the late nineteenth century at 30–35 cm at Isonzo, figures 3b and 4b). These shifts are best explained by the punctuation between two stasis segments or by the

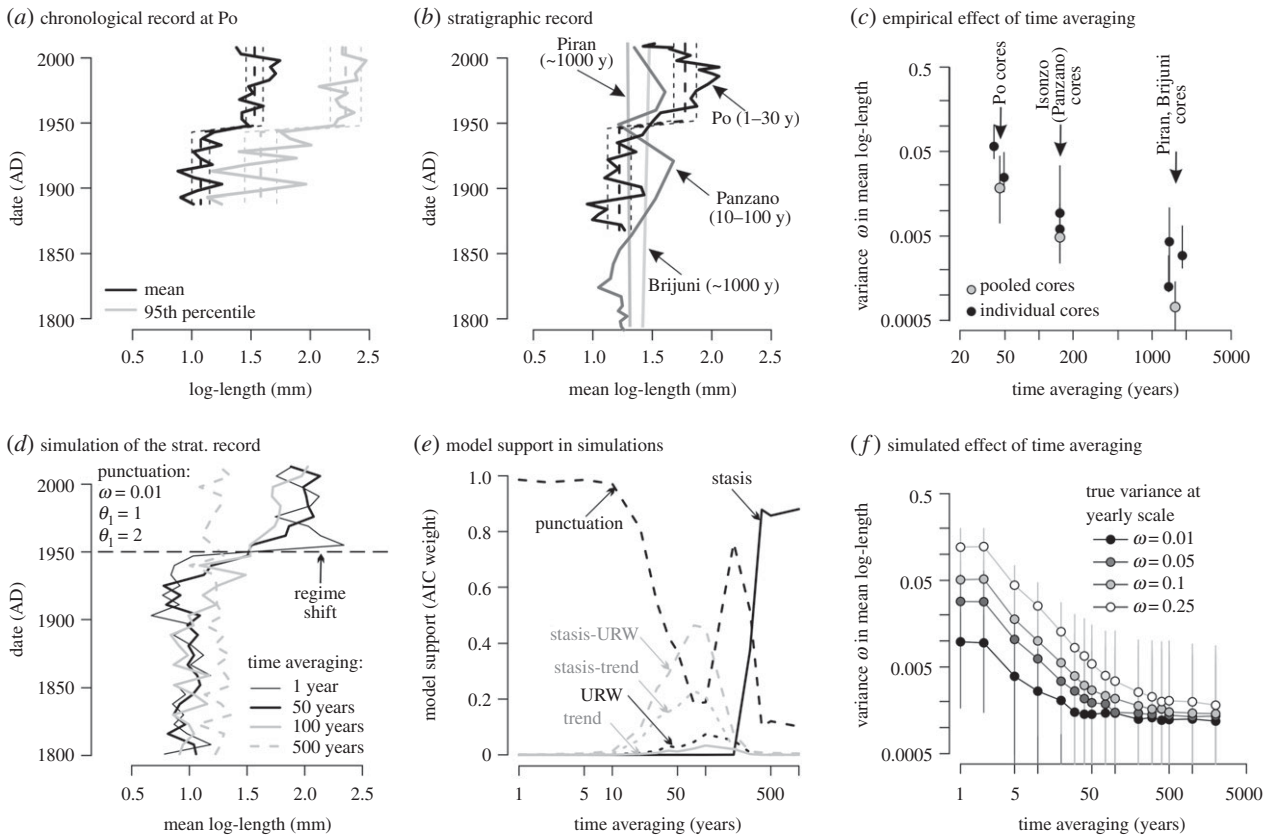


Figure 4. The sensitivity of the stratigraphic record of size shifts to empirical and simulated time averaging. (a) The chronological record demonstrates a punctuation in the mean and 95th percentile log-length at Po in the mid-twentieth century. (b) The stratigraphic records in the mean log-length at sites differing in time averaging (IQR in brackets), with date (AD) on the y-axis corresponding to the median date of individual increments. The black dashed line in (a) and (b) is the fit for the Po prodelta based on the threshold regression. The Piran and Brijuni records are effectively straight lines that cannot be resolved owing to condensation—the topcore increment (approx. 2013 AD) is connected with the underlying increment with median age older than 200 years. (c) The negative relationship between time averaging and the variance in mean log-length (ω) observed in the HST increments. ω (with 95% confidence intervals) was estimated at seven sites (two cores at Po, Isonzo, Piran, and one core at Brijuni) and at three pooled sites (Po, Isonzo, Piran). (d) Simulated stratigraphic records of the regime shift in the mean log-length occurring in 1950 AD show that punctuation is replaced by gradual trends and by stasis as the level of time averaging is increased. (e) Based on (d), the punctuation model is supported at decadal time averaging, random walks and directional trends at time averaging reaching 50–200 years, and stasis at greater than 200 years. (f) The negative relationship between time averaging and ω predicted in Holocene-scale simulations, in accord with empirical observations in (c). Temporal volatility in the mean log-length is thus expected to be severely reduced under centennial and millennial time averaging.

shift from stasis to random walk (figure 3b) and thus capture similar dynamics as the chronological records. By contrast, stratigraphic records at sites with low sedimentation rates (approx. 0.01 cm y^{-1}) either detect a size decline between the TST and HST assemblages or do not show any shifts, and produce estimates of ω that are smaller than at Po and Isonzo (figure 4c). Although the signature of the size increase in the twentieth century is mostly lost at these sites, it is still partly preserved by heavy-tailed distributions of the strongly time-averaged mixtures of highstand and Anthropocene shells, which are distinct from the TST and HST assemblages that are consistently dominated by small-size individuals (figure 1b). These heavy-tailed assemblages become bimodal when old shells without the surficial periostracum layer are excluded (electronic supplementary material, figure S2 and S3). Therefore, body size changes during the Holocene until the twentieth century are of smaller magnitude than the size increase observed in the twentieth century.

Although the Po and Isonzo records with the upcore transition from centennial to decadal averaging in the twentieth century deposits capture the abrupt increase in size relatively well, size changes at sites with millennial averaging are very muted and support a single stasis model (figure 3b). This difference in the stratigraphic expression of size pattern is confirmed by simulations of abrupt size increase in 1950 AD,

which predict that the punctuation is preserved when the magnitude of time averaging does not exceed approximately 20–50 years (figure 4d,e). The variance (ω) in the mean and in the 95th percentile log-length declines by two orders of magnitude with time averaging increasing from decadal to millennial values, both in the empirical and simulated stratigraphic records (figure 4c,f). Time averaging thus pulls the size trajectory in the stratigraphic record towards stronger stasis and towards very small ω at sites with slow sedimentation. This effect is limited at Po and Isonzo because punctuations at these sites on the transition to the Anthropocene increments coincide with a two- to threefold decline in time averaging: from 25–50 to approximately 10–30 years at Po and from 75 to approximately 10–20 years at Isonzo (figure 2). The stratigraphic records at the Po and Isonzo prodeltas thus distinctly preserve the twentieth century regime shift under high or moderate sediment accumulation rates because time averaging of the late twentieth century assemblages is reduced.

4. Discussion

Corbula gibba size increased abruptly from 5 to 10–15 mm in the whole northern Adriatic Sea during the twentieth century, contrasting starkly with the rarity of such large specimens in

the pre-Anthropocene record (figures 1a, 2a,b). This change in size distribution of the dominant species reflects a community-wide regime shift, because it was associated with a major turnover in both taxonomic and functional composition of the molluscan assemblages (figure 2c,d, electronic supplementary material, figure S7). Although *C. gibba* was a persistent subset of molluscan communities during the Holocene [45,46], it became dominant relative to molluscan suspension feeders and other functional groups in the twentieth century (electronic supplementary material, figure S7). The bimodality of abundances of *C. gibba* prior to and after the transition in the twentieth century (with modes at approximately 20% and 90%, respectively; figure 2d) is diagnostic of an abrupt ecological transition [47]. The latest twentieth century LAs still differs from the time-averaged Anthropocene DAs. The intermediate position of Anthropocene DAs between the older Holocene assemblages and Anthropocene LAs (figure 2c,e) thus indicating that even at Po and Isonzo prodeltas where sedimentation rates are relatively high, the proportional abundance of *C. gibba* in DAs is still reduced by the mixing with older shells from other molluscan species.

Several lines of evidence indicate that the regime shift was driven by a transition towards higher frequency of seasonal hypoxia. First, the increase in size and dominance of *C. gibba* coincided with the late twentieth century eutrophication coupled with a general increase in the frequency of hypoxic events [48]. Although seasonal hypoxia occasionally affected benthic communities also prior to the twentieth century, the recurrence of hypoxic events was less frequent [34]. Second, *C. gibba* populations that did not experience an increase in size during the twentieth century were limited to the shallowest or high-energy habitats at the Isonzo prodelta and off Venice. They were thus not subjected to seasonal hypoxia, in contrast with deeper habitats located below the thermocline and experiencing annual to inter-annual frequencies of hypoxic events at the Po prodelta [49] and less regular hypoxic events in the Gulf of Trieste [50]. Third, size in DAs increases geographically with the relative frequency of seasonal hypoxia at 16 sites (figure 2b). The abrupt increase in the 95th percentile log-length at sites with at least one hypoxic event per decade indicates that the shift between the two states follows a threshold-type dynamic [11].

Direct biological observations showed that seasonal mass mortalities in the late twentieth century in the Adriatic Sea negatively affected predators and substrate-destabilizing bioturbators, including burrowing shrimps, infaunal echinoids, holothurians, predatory asteroids and muricid gastropods [51]. The recovery of these taxa in the wake of hypoxic events in the northern Adriatic Sea is delayed and occurs over several years [52]. This allows *C. gibba* with hypoxia tolerance [53] and with rapid re-colonization potential [54–57] to dominate benthic communities also in years with persistently normoxic conditions. We thus hypothesize that the increase in body size and dominance of *C. gibba*, both responding to the shift of the northern Adriatic to higher frequency of disturbance by hypoxia, is driven by ecological release [58] from predation, competition and trophic amensalism. This release hypothesis is congruent with the decline in abundance of predatory gastropods observed here and with a major decline in abundance of bulldozing infaunal echinoids (that can negatively affect slow-burrowing bivalves such as *C. gibba*), which was observed in the northern Adriatic Sea during the late twentieth century [59,60].

As can be expected, low sedimentation rates that lead to multi-decadal or millennial time averaging will strongly reduce temporal variance in body size and will bias abrupt shifts towards gradual trends. However, high sedimentation rates (greater than 0.2 cm y^{-1}) are also not sufficient for the preservation of high-resolution ecological dynamics in the fossil record if associated with deep sediment mixing by bioturbation. Time averaging of the present-day 10–20 cm thick mixed layer [34,61] can be expected to be approximately 10–20 years under sedimentation rates of 1 cm y^{-1} at Po prodelta, which is consistent with the observed values of time averaging in the late twentieth century sediments. However, time averaging of approximately 25–50 years, the lack of preservation of flood layers and stronger mottling in pre-Anthropocene sediments at the Po and Isonzo prodeltas indicate that the thickness of the mixed layer exceeded approximately 25 cm prior to 1950 AD [34,62]. This decline in time averaging was not associated with an increase in sedimentation rates. Therefore, under naturally deeper sediment mixing prior to anthropogenic increase in hypoxia, multi-decadal time averaging would obliterate the stratigraphic signal of abrupt ecological shifts even under high sedimentation rates (figure 4d,e).

The temporal association of the size and compositional changes in the molluscan community with the declining bioturbation indicates a common cause behind the regime shift and its increased preservation potential in the fossil record. The preservation of abrupt regime shifts in the stratigraphic record is triggered by the pervasive ecosystem change of decadal-scale duration that is associated with the decline in the depth of sediment mixing by burrowers, especially in settings with high to moderate net accumulation rates and without long hiatuses. The Anthropocene regime shift in the macrobenthic communities in the northern Adriatic Sea is not only unprecedented relative to the Holocene history but is also sufficiently strong and temporally persistent to be distinctly preserved in the stratigraphic record, paralleling Anthropocene shifts in microbiotic proxies documented in marginal marine environments [63,64]. The differences in the intensity of bioturbation between (i) perturbation regimes with limited mixing by bioturbation and (ii) background regimes with intense and deep mixing by bioturbation can thus generate a dichotomy in the resolution of the marine fossil record on continental shelves. On one hand, the majority of the fossil record that formed in shelf ecosystems with intense bioturbation is probably averaged to centuries or millennia and rich in gaps [65], as is also observed in the northern Adriatic Sea [66,67]. On the other hand, the window for preservation of highly resolved ecological dynamic opens in the aftermath of anoxic and hypoxic events (leading to limited or totally absent bioturbation, [68–71]) on the present-day marine shelves and was probably open in the wake of major ecosystem perturbations in the geological past [73–74].

Data accessibility. Body size and compositional data, and R language codes are available from the Dryad Digital Repository: <https://doi.org/10.5061/dryad.t4b8gthzr> [29].

Authors' contributions. A.T. and M.Z. designed the research, P.G.A., T.F., I.G., A.H., M.K., R.N., V.N. and D.S. collected the data, A.T. compiled and analysed the data, and all authors discussed the results and contributed to the writing of the manuscript.

Competing interests. We declare we have no competing interests.

Funding. This study was funded by the Austrian Science Fund (FWF project P24901), the Slovak Scientific Grant Agency (VEGA 0169-19), Slovak Research and Development Agency (APVV17-0555) and the National Science Foundation (EAR-0920075 and EAR-1559196).

Acknowledgements. The authors thank S.M. Holland, E. Edinger and an anonymous referee for critical comments.

- Petersen JK, Hansen JW, Laursen MB, Clausen P, Carstensen J, Conley DJ. 2008 Regime shift in a coastal marine ecosystem. *Ecol. Appl.* **18**, 497–510. (doi:10.1890/07-0752.1)
- Villnäs A, Norkko A. 2011 Benthic diversity gradients and shifting baselines: implications for assessing environmental status. *Ecol. Appl.* **21**, 2172–2186. (doi:10.1890/10-1473.1)
- Rombouts I *et al.* 2013 Evaluating marine ecosystem health: case studies of indicators using direct observations and modelling methods. *Ecol. Indic.* **24**, 353–365. (doi:10.1016/j.ecolind.2012.07.001)
- Di Camillo CG, Cerrano C. 2015 Mass mortality events in the NW Adriatic Sea: phase shift from slow-to fast-growing organisms. *PLoS ONE* **10**, e0126689. (doi:10.1371/journal.pone.0126689)
- Dornelas M, Gotelli NJ, Shimadzu H, Moyes F, Magurran AE, McGill BJ. 2019 A balance of winners and losers in the Anthropocene. *Ecol. Lett.* **22**, 847–854. (doi:10.1111/ele.13242)
- Chase JM *et al.* 2019 Species richness change across spatial scales. *Oikos* **128**, 1079–1091. (doi:10.1111/oik.05968)
- Rocha J, Yletyinen J, Biggs R, Blenckner T, Peterson G. 2015 A holistic view of marine regime shifts. *Phil. Trans. R. Soc. B* **370**, 20130273. (doi:10.1098/rstb.2013.0273)
- Aronson RB, Macintyre IG, Wapnick CM, O'Neill MW. 2004 Phase shifts, alternative states, and the unprecedented convergence of two reef systems. *Ecology* **85**, 1876–1891. (doi:10.1890/03-0108)
- Pandolfi JM, Jackson JB. 2006 Ecological persistence interrupted in Caribbean coral reefs. *Ecol. Lett.* **9**, 818–826. (doi:10.1111/j.1461-0248.2006.00933.x)
- Kidwell SM. 2007 Discordance between living and death assemblages as evidence for anthropogenic ecological change. *Proc. Natl Acad. Sci. USA* **104**, 17 701–17 706. (doi:10.1073/pnas.0707194104)
- Williams JW, Blois JL, Shuman BN. 2011 Extrinsic and intrinsic forcing of abrupt ecological change: case studies from the late Quaternary. *J. Ecol.* **99**, 664–677. (doi:10.1111/j.1365-2745.2011.01810.x)
- Tomašových A, Kidwell SM. 2017 Nineteenth-century collapse of a benthic marine ecosystem on the open continental shelf. *Proc. R. Soc. B* **284**, 20170328. (doi:10.1098/rspb.2017.0328)
- Keller G, Mateo P, Punekar J, Khozyem H, Gertsch B, Spangenberg J, Bitchong AM, Adatte T. 2018 Environmental changes during the Cretaceous–Paleogene mass extinction and Paleocene–Eocene thermal maximum: implications for the Anthropocene. *Gandwana Res.* **56**, 69–89. (doi:10.1016/j.gr.2017.12.002)
- Aberhan M, Kiessling W. 2015 Persistent ecological shifts in marine molluscan assemblages across the end-Cretaceous mass extinction. *Proc. Natl Acad. Sci. USA* **112**, 7207–7212. (doi:10.1073/pnas.1422248112)
- Penn JL, Deutsch C, Payne JL, Sperling EA. 2018 Temperature-dependent hypoxia explains biogeography and severity of end-Permian marine mass extinction. *Science* **362**, eaat1327. (doi:10.1126/science.aat1327)
- Kosnik MA, Hua Q, Jacobsen GE, Kaufman DS, Wüst RA. 2007 Sediment mixing and stratigraphic disorder revealed by the age-structure of *Tellina* shells in Great Barrier Reef sediment. *Geology* **35**, 811–814. (doi:10.1130/G23722A.1)
- Tomašových A, Kidwell SM. 2010 The effects of temporal resolution on species turnover and on testing metacommunity models. *Am. Nat.* **175**, 587–606. (doi:10.1086/651661)
- Rabalais NN, Turner RE, Gupta BKS, Platon E, Parsons ML. 2007 Sediments tell the history of eutrophication and hypoxia in the northern Gulf of Mexico. *Ecol. Appl.* **17**, S129–S143. (doi:10.1890/06-0644.1)
- Seddon AW, Froyd CA, Witkowski A, Willis KJ. 2014 A quantitative framework for analysis of regime shifts in a Galápagos coastal lagoon. *Ecology* **95**, 3046–3055. (doi:10.1890/13-1974.1)
- Jonkers L, Hillebrand H, Kucera M. 2013 Global change drives modern plankton communities away from the pre-industrial state. *Nature* **570**, 372–375. (doi:10.1038/s41586-019-1230-3)
- Kidwell SM. 1998 Time-averaging in the marine fossil record: overview of strategies and uncertainties. *Geobios* **30**, 977–995. (doi:10.1016/S0016-6995(97)80219-7)
- Leonard-Pingel JS, Kidwell SM, Tomašových A, Alexander CR, Cadien DB. 2019 Gauging benthic recovery from 20th century pollution on the southern California continental shelf using bivalves from sediment cores. *Mar. Ecol. Prog. Ser.* **615**, 101–119. (doi:10.3354/meps12918)
- Kemp DB, Eichenseer K, Kiessling W. 2015 Maximum rates of climate change are systematically underestimated in the geological record. *Nat. Commun.* **6**, 8890. (doi:10.1038/ncomms9890)
- Holland SM. 2016 The non-uniformity of fossil preservation. *Phil. Trans. R. Soc. B* **371**, 20150130. (doi:10.1098/rstb.2015.0130)
- Martindale RC, Aberhan M. 2017 Response of macrobenthic communities to the Toarcian Oceanic Anoxic Event in northeastern Panthalassa (Ya Ha Tinda, Alberta, Canada). *Palaeogeogr. Palaeoclimatol. Palaeoecol.* **478**, 103–120. (doi:10.1016/j.palaeo.2017.01.009)
- Foster WJ *et al.* 2020 Evolutionary and ecophenotypic controls on bivalve body size distributions following the end-Permian mass extinction. *Glob. Planet Change* **185**, 103088. (doi:10.1016/j.gloplacha.2019.103088)
- Levin LA, Ekau W, Gooday AJ, Jorissen F, Middelburg JJ, Naqvi SWA, Neira C, Rabalais NN, Zhang J. 2009 Effects of natural and human-induced hypoxia on coastal benthos. *Biogeosciences* **6**, 2063–2098. (doi:10.5194/bg-6-2063-2009)
- Payne JL, Bush AM, Heim NA, Knope ML, Mccauley DJ. 2016 Ecological selectivity of the emerging mass extinction in the oceans. *Science* **353**, 1284–1286. (doi:10.1126/science.aaf2416)
- Tomašových A *et al.* 2020 Data from: Ecological regime shift preserved in the Anthropocene Stratigraphic record. Dryad Digital Repository. (<https://doi.org/10.5061/dryad.t4b8gthzr>)
- Dornelas M *et al.* 2013 Quantifying temporal change in biodiversity: challenges and opportunities. *Proc. R. Soc. B* **280**, 20121931. (doi:10.1098/rspb.2012.1931)
- Hunt G. 2008 Gradual or pulsed evolution: when should punctuational explanations be preferred? *Paleobiology* **34**, 360–377. (doi:10.1666/07073.1)
- Sessa JA, Bralower TJ, Patzkowsky ME, Handley JC, Ivany LC. 2012 Environmental and biological controls on the diversity and ecology of Late Cretaceous through early Paleogene marine ecosystems in the US Gulf Coastal Plain. *Paleobiology* **38**, 218–239. (doi:10.1666/10042.1)
- Amorosi A, Centineo MC, Colalongo ML, Pasini G, Sarti G, Vaiani SC. 2003 Facies architecture and latest Pleistocene–Holocene depositional history of the Po Delta (Comacchio area), Italy. *J. Geol.* **111**, 39–56. (doi:10.1086/344577)
- Tomašových A, Gallmetzer I, Haselmair A, Kaufman DS, Kralj M, Cassin D, Zonta R, Zuschin M. 2018 Tracing the effects of eutrophication on molluscan communities in sediment cores: outbreaks of an opportunistic species coincide with reduced bioturbation and high frequency of hypoxia in the Adriatic Sea. *Paleobiology* **44**, 575–602. (doi:10.1017/pab.2018.22)
- Tomašových A, Gallmetzer I, Haselmair A, Kaufman DS, Mavrič B, Zuschin M. 2019 A decline in molluscan carbonate production driven by the loss of vegetated habitats encoded in the Holocene sedimentary record of the Gulf of Trieste. *Sedimentology* **66**, 781–807. (doi:10.1111/sed.12516)
- Tomašových A, Gallmetzer I, Haselmair A, Kaufman DS, Vidović J, Zuschin M. 2017 Stratigraphic unmixing reveals repeated hypoxia events over the past 500 yr in the northern Adriatic Sea. *Geology* **45**, 363–366. (doi:10.1130/G38676.1)
- Gallmetzer I, Haselmair A, Tomašových A, Mautner AK, Schnedl SM, Cassin D, Zonta R, Zuschin M. 2019 Tracing origin and collapse of Holocene benthic baseline communities in the northern Adriatic. *Palaio* **34**, 121–145. (doi:10.2110/palo.2018.068)
- Steckbauer A, Duarte CM, Carstensen J, Vaquer-Sunyer R, Conley DJ. 2011 Ecosystem impacts of hypoxia: thresholds of hypoxia and pathways to recovery. *Environ. Res. Lett.* **6**, 025003. (doi:10.1088/1748-9326/6/2/025003)
- Simpson GL. 2007 Analogue methods in palaeoecology: using the analogue package. *J. Stat. Softw.* **22**, 1–29. (doi:10.18637/jss.v022.i02)
- Scarponi D, Kaufman D, Amorosi A, Kowalewski M. 2013 Sequence stratigraphy and the resolution of

- the fossil record. *Geology* **41**, 239–242. (doi:10.1130/G33849.1)
41. Albano PG, Gallmetzer I, Haselmair A, Tomašových A, Stachowitsch M, Zuschin M. 2018 Historical ecology of a biological invasion: the interplay of eutrophication and pollution determines time lags in establishment and detection. *Biol. Invasions* **20**, 1417–1430. (doi:10.1007/s10530-017-1634-7)
 42. Goberville E, Beaugrand G, Sautour B, Tréguer P. 2011 Evaluation of coastal perturbations: a new mathematical procedure to detect changes in the reference state of coastal systems. *Ecol. Indic.* **11**, 1290–1300. (doi:10.1016/j.ecolind.2011.02.002)
 43. Tomašových A, Kidwell SM. 2011 Accounting for the effects of biological variability and temporal autocorrelation in assessing the preservation of species abundance. *Paleobiology* **37**, 332–354. (doi:10.1666/09506.1)
 44. Anderson MJ, Walsh DC. 2013 PERMANOVA, ANOSIM, and the Mantel test in the face of heterogeneous dispersions: what null hypothesis are you testing? *Ecol. Monogr.* **83**, 557–574. (doi:10.1890/12-2010.1)
 45. Scarponi D, Kowalewski M. 2007 Sequence stratigraphic anatomy of diversity patterns: Late Quaternary benthic mollusks of the Po Plain, Italy. *Palaios* **22**, 296–305. (doi:10.2110/palo.2005.p05-020r)
 46. Kowalewski M, Wittmer JM, Dexter TA, Amorosi A, Scarponi D. 2015 Differential responses of marine communities to natural and anthropogenic changes. *Proc. R. Soc. B* **282**, 20142990. (doi:10.1098/rspb.2014.2990)
 47. Bestelmeyer BT *et al.* 2011 Analysis of abrupt transitions in ecological systems. *Ecosphere* **2**, 1–26. (doi:10.1890/ES11-00216.1)
 48. Justić D. 1991 Hypoxic conditions in the northern Adriatic Sea: historical development and ecological significance. *Geol. Soc. Spec. Publ.* **58**, 95–105. (doi:10.1144/GSL.SP.1991.058.01.07)
 49. Alvisi F, Cozzi S. 2016 Seasonal dynamics and long-term trend of hypoxia in the coastal zone of Emilia Romagna (NW Adriatic Sea, Italy). *Sci. Total Environ.* **541**, 1448–1462. (doi:10.1016/j.scitotenv.2015.10.011)
 50. Kralj M, Lipizer M, Čermelj B, Celio M, Fabbro C, Brunetti F, France J, Mozetič P, Giani M. 2019 Hypoxia and dissolved oxygen trends in the northeastern Adriatic Sea (Gulf of Trieste). *Deep Sea Res. Part II* **164**, 74–88. (doi:10.1016/j.dsr2.2019.06.002)
 51. Stachowitsch M. 1984 Mass mortality in the Gulf of Trieste: the course of community destruction. *Mar. Ecol.* **5**, 243–264. (doi:10.1111/j.1439-0485.1984.tb00124.x)
 52. Hrs-Brenko M. 2006 The basket shell, *Corbula gibba* Olivi, 1792 (bivalve mollusks) as a species resistant to environmental disturbances: a review. *Acta Adriatica* **47**, 49–64.
 53. Riedel B, Pados T, Pretreberner K, Schiemer L, Steckbauer A, Haselmair A, Zuschin M, Stachowitsch M. 2014 Effect of hypoxia and anoxia on invertebrate behaviour: ecological perspectives from species to community level. *Biogeosciences* **11**, 1491–1518. (doi:10.5194/bg-11-1491-2014)
 54. Borja A, Franco J, Pérez V. 2000 A marine biotic index to establish the ecological quality of soft-bottom benthos within European estuarine and coastal environments. *Mar. Poll. Bull.* **40**, 1100–1114. (doi:10.1016/S0025-326X(00)00061-8)
 55. Simonini R, Grandi V, Massamba-N'Siala G, Iotti M, Montanari G, Prevedelli D. 2009 Assessing the ecological status of the north-western Adriatic Sea within the European Water Framework Directive: a comparison of Bentix, AMBI and M-AMBI methods. *Mar. Ecol.* **30**, 241–254. (doi:10.1111/j.1439-0485.2009.00281.x)
 56. Paganelli D, Marchini A, Occhipinti-Ambrogi A. 2012 Functional structure of marine benthic assemblages using biological traits analysis (BTA): a study along the Emilia-Romagna coastline (Italy, North-West Adriatic Sea). *Estuarine Coastal Shelf Sci.* **96**, 245–256. (doi:10.1016/j.ejss.2011.11.014)
 57. Solis-Weiss V, Aleffi F, Bettoso N, Rossin P, Orel G, Fonda-Umani S. 2004 Effects of industrial and urban pollution on the benthic macrofauna in the Bay of Muggia (industrial port of Trieste, Italy). *Sci. Total Environ.* **328**, 247–263. (doi:10.1016/j.scitotenv.2004.01.027)
 58. Yoder JB *et al.* 2010 Ecological opportunity and the origin of adaptive radiations. *J. Evol. Biol.* **23**, 1581–1596. (doi:10.1111/j.1420-9101.2010.02029.x)
 59. Schinner F, Stachowitsch M, Hilgers H. 1996 Loss of benthic communities: warning signal for coastal ecosystem management. *Aquat. Conserv. Mar. Freshwater Ecosyst.* **6**, 343–352. (doi:10.1002/(SICI)1099-0755(199612)6:4<343::AID-AQC196>3.0.CO;2-B)
 60. Chiantore M, Bedulli D, Cattaneo-Vietti R, Schiaparelli S, Albertelli G. 2001 Long-term changes in the mollusc-echinoderm assemblages in the north and coastal middle Adriatic Sea. *Atti. Ital. Ocean Limn.* **14**, 63–75.
 61. Tesi T, Langone L, Goñi, Wheatcroft RA, Miserocchi S, Bertotti L. 2012 Early diagenesis of recently deposited organic matter: a 9-yr time-series study of a flood deposit. *Geochim. Cosmochim. Acta* **83**, 19–36. (doi:10.1016/j.gca.2011.12.026)
 62. Covelli S, Fontolan G, Faganelli J, Ogrinc N. 2006 Anthropogenic markers in the Holocene stratigraphic sequence of the Gulf of Trieste (northern Adriatic Sea). *Mar. Geol.* **230**, 29–51. (doi:10.1016/j.margeo.2006.03.013)
 63. Waters CN *et al.* 2016 The Anthropocene is functionally and stratigraphically distinct from the Holocene. *Science* **351**, aad2622. (doi:10.1126/science.aad2622)
 64. Wilkinson IP, Poirier C, Head MJ, Sayer CD, Tibby J. 2014 Microbiotic signatures of the Anthropocene in marginal marine and freshwater palaeoenvironments. *Geol. Soc. Spec. Publ.* **395**, 185–219. (doi:10.1144/SP395.14)
 65. Holland SM, Patzkowsky ME. 2015 The stratigraphy of mass extinction. *Palaeontology* **58**, 903–924. (doi:10.1111/pala.12188)
 66. Novak A, Šmuc A, Poglajen S, Vrabec M. 2020 Linking the high-resolution acoustic and sedimentary facies of a transgressed Late Quaternary alluvial plain (Gulf of Trieste, northern Adriatic). *Mar. Geol.* **419**, 106061. (doi:10.1016/j.margeo.2019.106061)
 67. Brunović D, Miko S, Hasan O, Papatheodorou G, Ilijanić N, Miserocchi S, Correggiari A, Geraga M. 2020 Late Pleistocene and Holocene paleoenvironmental reconstruction of a drowned karst isolation basin (Lošinj Channel, NE Adriatic Sea). *Palaeogeogr. Palaeoclimatol. Palaeoecol.* **544**, 109587. (doi:10.1016/j.palaeo.2020.109587)
 68. Dashtgard SE, Snedden JW, MacEachern JA. 2015 Unbioturbated sediments on a muddy shelf: hypoxia or simply reduced oxygen saturation? *Palaeogeogr. Palaeoclimatol. Palaeoecol.* **425**, 128–138. (doi:10.1016/j.palaeo.2015.02.033)
 69. Jokinen SA *et al.* 2018 A 1500-year multiproxy record of coastal hypoxia from the northern Baltic Sea indicates unprecedented deoxygenation over the 20th century. *Biogeosciences* **15**, 3975–4001. (doi:10.5194/bg-15-3975-2018)
 70. Virtasalo JJ, Kotilainen AT, Gingras MK. 2006. Trace fossils as indicators of environmental change in Holocene sediments of the Archipelago Sea, northern Baltic Sea. *Palaeogeogr. Palaeoclimatol. Palaeoecol.* **240**, 453–467. (doi:10.1016/j.palaeo.2006.02.010)
 71. Caswell BA, Coe AL. 2013 Primary productivity controls on opportunistic bivalves during Early Jurassic oceanic deoxygenation. *Geology* **41**, 1163–1166. (doi:10.1130/G34819.1)
 72. Hofmann RL, Buatois LA, Macnaughton RB, Mángano MG. 2015 Loss of the sedimentary mixed layer as a result of the end-Permian extinction. *Palaeogeogr. Palaeoclimatol. Palaeoecol.* **428**, 1–11. (doi:10.1016/j.palaeo.2015.03.036)
 73. Danise S, Twitchett RJ, Little CT 2015. Environmental controls on Jurassic marine ecosystems during global warming. *Geology* **43**, 263–266. (doi:10.1130/G36390.1)
 74. Rodríguez-Tovar FJ, Miguez-Salas O, Duarte LV. 2017 Toarcian Oceanic Anoxic Event induced unusual behaviour and palaeobiological changes in *Thalassinoides* tracemakers. *Palaeogeogr. Palaeoclimatol. Palaeoecol.* **485**, 46–56. (doi:10.1016/j.palaeo.2017.06.002)